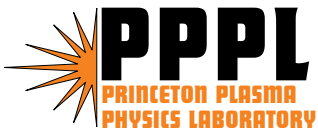# Princeton Plasma Physics Laboratory

Advanced ST Plasma Scenario Simulations for NSTX

C.E. Kessel, E.J. Synakowski, D.A. Gates, R.W. Harvey,
S.M. Kaye, T.K. Mau, J. Menard, C.K. Phillips, G. Taylor,
R. Wilson, and the NSTX Research Team

October 2004

PPPL Report Disclaimers

Full Legal Disclaimer

Trademark Disclaimer

PPPL Report Availability

Advanced ST Plasma Scenario Simulations for NSTX

C. E. Kessel, E. J. Synakowski, D. A. Gates, R. W. Harvey[1], S. M. Kaye, T. K. Mau[2], J. Menard, C. K. Phillips, G. Taylor, R. Wilson and the NSTX Research Team

Princeton Plasma Physics Laboratory, Princeton, NJ, USA

[1]CompX, Del Mar, CA, USA

[2]University of California, San Diego, CA, USA

ckessel@pppl.gov

Abstract. Integrated scenario simulations are done for NSTX that address four primary milestones for developing advanced ST configurations: high β and high β_N inductive discharges to study all aspects of ST physics in the high beta regime; non-inductively sustained discharges for flattop times greater than the skin time to study the various current drive techniques; non-inductively sustained discharges at high β for flattop times much greater than a skin time which provides the integrated advanced ST target for NSTX; and non-solenoidal startup and plasma current rampup. The simulations done here use the Tokamak Simulation Code (TSC) and are based on a discharge 109070. TRANSP analysis of the discharge provided the thermal diffusivities for electrons and ions, the neutral beam (NB) deposition profile and other characteristics. CURRAY is used to calculate the High Harmonic Fast Wave (HHFW) heating depositions and current drive. GENRAY/CQL3D is used to establish the heating and CD deposition profiles for electron Bernstein waves (EBW). Analysis of the ideal MHD stability is done with JSOLVER, BALMSC, and PEST2. The simulations indicate that the integrated advanced ST plasma is reachable, obtaining stable plasmas with $\beta \approx 40\%$ at β_N's of 7.7-9, $I_P = 1.0$ MA and $B_T = 0.35$ T. The plasma is 100% non-inductive and has a flattop of 4 skin times. The resulting global energy confinement corresponds to a multiplier of $H_{98(y,2)} = 1.5$. The simulations have demonstrated the importance of HHFW heating and CD, EBW off-axis CD, strong plasma shaping, density control, and early heating/H-mode transition for producing and optimizing these plasma configurations

1. Introduction

The spherical torus concept will provide an attractive fusion energy configuration if it can demonstrate the following major features: high plasma elongation with significant triangularity, 100% non-inductive current with a credible path to high bootstrap current fractions, non-solenoidal startup/rampup of the plasma current, high β with stabilization of the RWM instabilities, and sufficiently high energy confinement. Demonstrating these features experimentally will likely be achieved individually, and then simultaneously to varying degrees. Integrated scenario modeling is a key element to guide experiments toward achieving these features.

The long term planning for NSTX integrated scenario modeling involves a sequence of goals aligned with the experimental milestones[1-3]. These include the following: high β operation with $\beta_N > 8$ for $\tau_{flat} > \tau_E$, 100% non-inductive operation for $\tau_{flat} > \tau_{skin}$, the integrated goal of 100% non-inductive high β operation with $\beta_N > 8$ for $\tau_{flat} \gg \tau_{skin}$, and non-solenoidal plasma startup and current rampup. The first goal represents the transient optimization of β under various conditions and will not be reported in this paper.

Predictive simulations are done with the Tokamak Simulation Code (TSC) [4], in combination with other analysis, to find ways to produce these plasmas based on experimental data and self-consistent integrated modeling.

2. Computational Approach

The time-dependent computer codes used for integrated modeling are TSC and TRANSP[5]. The former provides free-boundary evolutions, while the latter provides fixed-boundary evolutions. TRANSP is used in the interpretive mode here to generate neutral beam (NB) characteristics and thermal diffusivities from the experiment. TSC is the predictive transport

code used as the backbone for the simulations reported in this paper. In addition, stand alone calculations are done, which rely on a static equilibrium, and are described below.

The CURRAY[6] code is used extensively to examine HHFW current drive under various situations in the scenarios. At present, beam energetic ion absorption is modeled by an equivalent Maxwellian distribution with a characteristic temperature and anisotropy. The GENRAY/CQL3D[7,8] codes are used to establish the EBW deposition and current drive. Some ideal MHD analysis will be given for selected scenario flattop plasmas. These are analyzed using an equilibrium description directly from TSC, which is read into the fixed boundary equilibrium code JSOLVER[9]. JSOLVER recalculates the equilibrium with high resolution for stability analysis. High-n ballooning stability is calculated with BALMSC[10], and n=1 external kink stability is assessed with PEST2[11]. By now it is well known that low aspect ratio plasmas require significant computational resolution, particularly for kink analysis, and the ideal MHD assessments made here are continuing.

The discharge 109070, which was NBI heated, is used as the basis for these simulation projections because it achieved 50% non-inductive current fraction, a β_N of 5.9, and an $H_{98(y,2)}$ value of 1.25. For this discharge I_P = 800 kA, B_T = 0.5 T, R = 0.88 m, a = 0.59 m, κ = 2.05, $\langle\delta\rangle$ = 0.45, β_N = 5.9, bootstrap current I_{BS} = 240 kA, I_{NB} = 160 kA, all evaluated at 450 ms.

For the simulations reported here the density profile and magnitude is prescribed as a function of time. The thermal diffusivities are taken from a TRANSP analysis of the discharge, 109070, and they are uniformly scaled according to IPB98(y,2) global energy confinement scaling. The beam heating profile is taken from TRANSP, with beam driven current calculated in TSC (which was benchmarked against the TRANSP result). Beam characteristics (beam stored energy, fast ion density, and deposition profile) are fixed to those of shot 109070, and scaled by the injected power. The Z_{eff} profile is taken from the experiment, having a hollow profile with a value of 2.5 at the plasma center and slightly over 4 at an r/a of 0.75. A benchmark discharge simulation is done with TSC of 109070 in order to match several parameters before proceeding with extrapolations. Profiles from the TSC simulation of 109070 are shown in Fig. 1.

3. Simulations of 100% Non-inductive Sustained Plasmas for $\tau_{flat} > \tau_{skin}$

The discharge simulations to produce 100% non-inductive current utilize 4 primary modifications to the base discharge 109070. These are 1) density control to reduce and maintain the density, 2) high elongation ($\approx$ 2.5) to maximize the bootstrap current fraction (Fig. 2), 3) early heating and H-mode transition, and 4) possible addition of HHFW power. The toroidal field is maintained at 0.5 T which has a maximum available flattop of 1.5 s. The plasma current was left at 800 kA.

Ideal MHD analysis of the several plasma equilibria from the TSC simulation of 109070 showed that the n=1 kink mode can have a significant internal component, which is not stabilized by a wall, in addition to the external component, even when the central safety factor was above 1.0. However this component did not exist when q(0) $\geq$ 1.5. Based on this, a rough goal of keeping the safety factor above 1.5 is adopted.

In the 2004 run campaign, experiments that combined NBI and HHFW indicated that it may be difficult to couple the HHFW power into the core plasma, and further research is required to resolve this. Due to these observations simulations are done both assuming no HHFW and including HHFW. In the former cases the total heating power is limited to about 5.5 M(from

NB's only) at 80 keV. The high elongation, density control, and early heating and H-mode were applied. It is found that due to the on-axis NBCD, the safety factor drops during the discharge, reaching 1.0 at 1.4 s into the discharge, and should be compared with the safety factor reaching 1.0 at about 550 ms in discharge 109070, representing a significant improvement. The predicted bootstrap and NB currents are each 355 kA, β_N reaches 4.7, the peak density is 0.3×10^{20} /m^3, the $H_{98(y,2)}$ factor is 1.23, and non-inductive current fraction is 92%. By enhancing the energy confinement multiplier to 1.5, or applying EBW (3 MW to produce 135 kA) current drive off-axis, the non-inductive current fraction reaches 100% and the safety factor is kept above 1.5 for the entire discharge, although it is still dropping very slowly. Results are shown in Fig. 3.
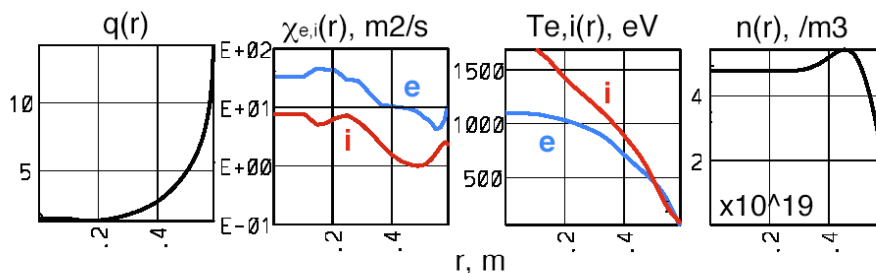

Figure 1. *Plasma profiles from the TSC simulation of the NSTX discharge 109070 at 450 ms, the thermal diffusivities are taken from the TRANSP reconstruction of the discharge.*

Significant flexibility can be gained if the HHFW is assumed to heat efficiently. Analysis with CURRAY indicated that a significant amount of power is absorbed on fast ions from the NB and thermal ions when $T_i/T_e > 1$, shown in Fig. 2. Since NBI discharges typically have $T_i/T_e \geq 2$, and CURRAY showed that only about 5 kA/MW would result over the entire $k_{\parallel}$ spectrum, no CD was assumed for HHFW, only heating. With 6 MW of HHFW heating and 4 MW of NB heating, which helped to reduce the on axis CD, the β_N reached 4.7, with 430 kA of bootstrap current and 355 kA of NB current. The non-inductive current fraction is 100%. The global energy confinement multiplier was 1.22, the plasma internal self-inductance li(1) was 0.57, and the peak density was 0.3×10^{20} /m^3. The safety factor remains above 2 throughout the discharge, and the available flattop time corresponds to 2 current diffusion times. This plasma is found to be stable to $n=\infty$ ballooning modes, except in the pedestal region, and $n=1$ with a wall located at 1.5a on the outboard only. Results are shown in Fig. 4, with additional cases showing the impact of lower Z_{eff} and broader NB current profile.
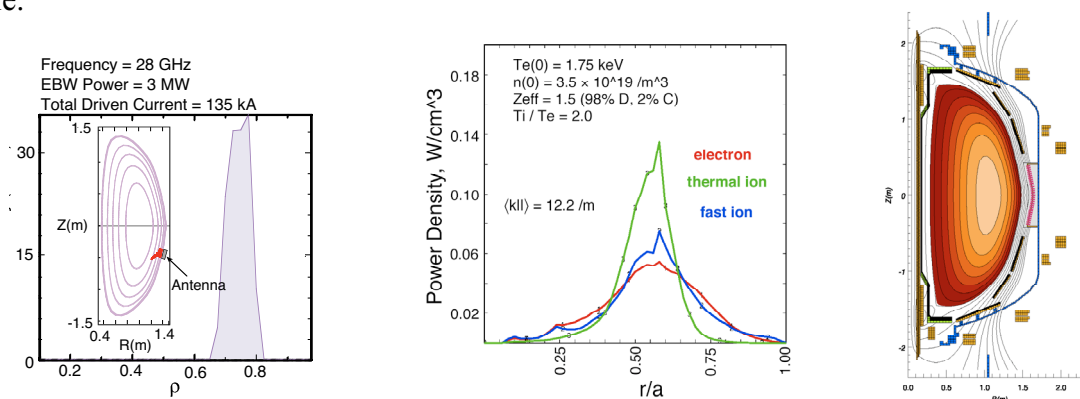
Figure 2. *EBW CD deposition calculated from GENRAY/CQL3D, HHFW power deposition on electrons, fast NB ions, and thermal ions calculated from CURRAY, and the simultaneous high κ and δ plasma shape that is used in scenario simulations and can be produced with a PF1A modification.*
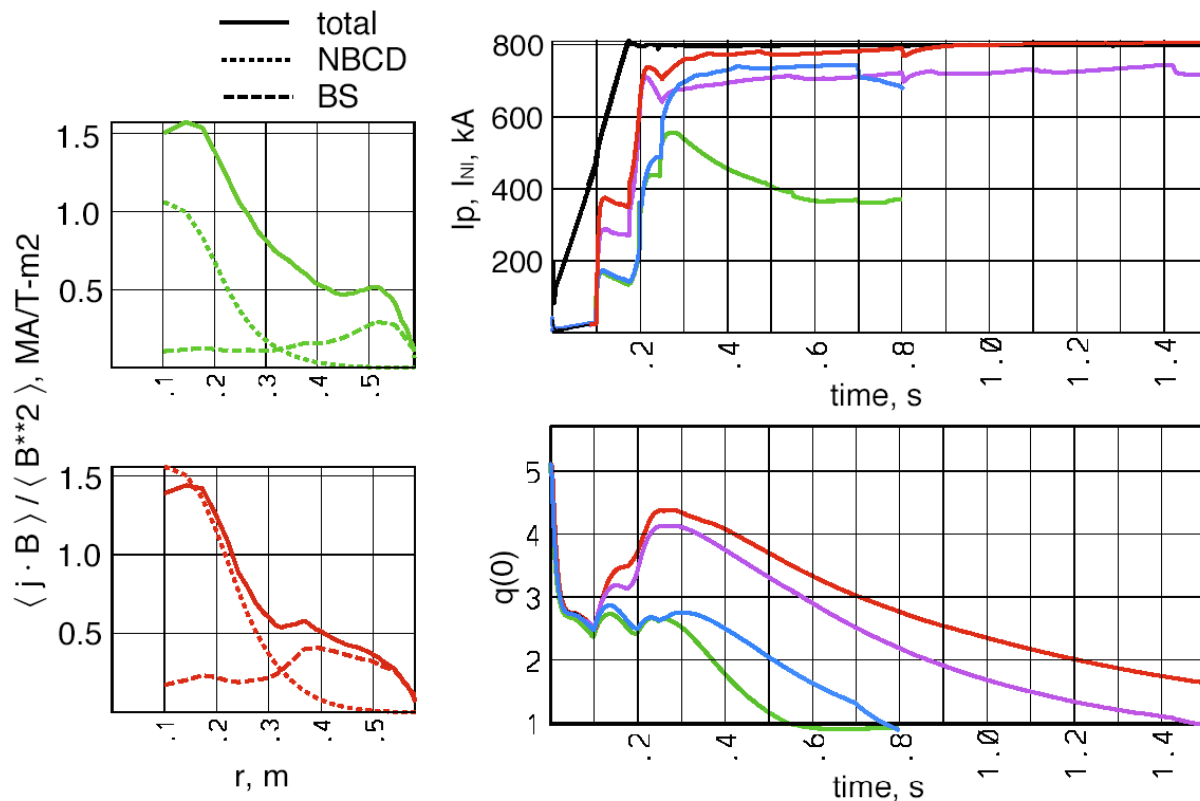
Figure 3. *Time histories of NBI-only 100% non-inductive scenarios, showing the central safety factor and the total non-inductive current for 109070 (green), high κ with density control (blue), high κ with density control and early heating H-mode (purple), and the same with slight enhancement in global energy confinement (red). The parallel current densities are shown for 109070 and the (red) case shown.*
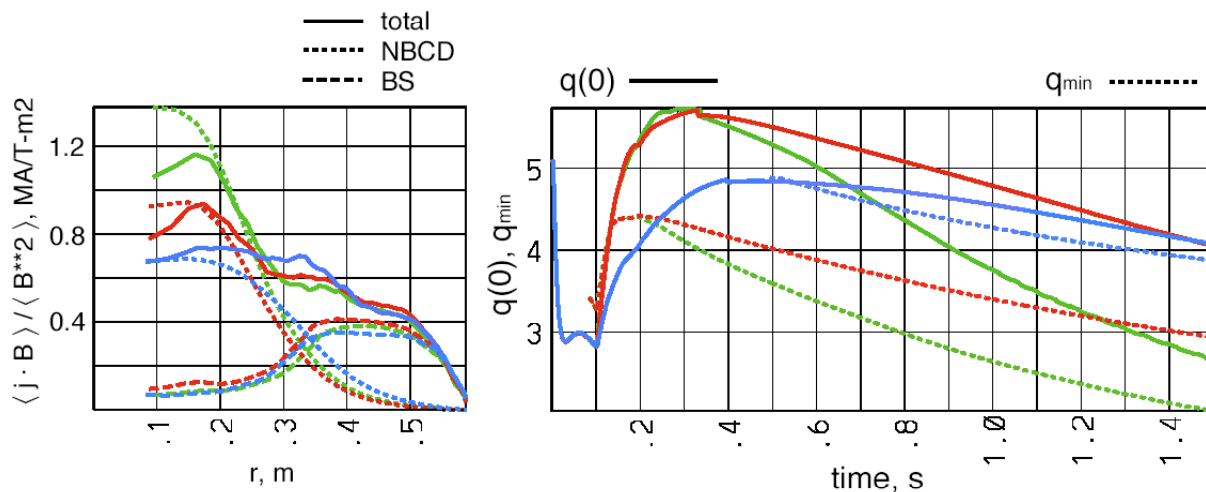
Figure 4. *Time histories of NBI and HHFW 100% non-inductive scenarios, showing the central and minimum safety factor, and parallel current densities for $P_{NB} = 4$ MW and $P_{HHFW} = 6$ MW, with high κ, density control, and early heating/H-mode (green), and lower Z_{eff} (red) or broader NB current distribution (blue).*

4. Simulations of 100% Non-inductive Sustained High β Plasmas for $\tau_{flat} \gg \tau_{skin}$

The integration goal for NSTX is to combine the 100% non-inductive sustainment and high β for times much longer than a current diffusion time, so as to produce an attractive plasma configuration that can be projected to steady state high fusion performance. Here the power and CD are provided by NB, HHFW, and EBW. Cases without HHFW will also be examined. The same primary features are applied here; 1) high elongation, 2) density control, 3) early heating and H-mode, and 4) the possible addition of HHFW. In addition, the toroidal field is lowered to 0.35-0.37 to access the high β, the plasma current was raised to 1.0 MA, and the EBW is considered fully developed to provide 3 MW of power delivered to the plasma. The decrease in the toroidal field and increase in plasma current are balanced against getting the various CD sources (including bootstrap) to provide the entire current and avoid the safety factor getting too low. The lower B_T allows the available flattop to increase to 3.5 s. Analysis with GENRAY/CQL3D (Fig. 2) showed that the EBW deposition was in the range of $0.6 \leq r/a \leq 0.85$, and could provide 45 kA/MW, with a frequency of 28 GHz and lower off-midplane launch[8].

Here we assume that no HHFW was included, so that NBI must provide all the central heating. In addition to the primary features listed above we include for these simulations higher NB energy of 100 keV giving 6.75 MW, higher energy confinement, and broader NB current profile based on lower B_T and higher Ip discharges. The bootstrap current is 460 kA, the NB current is 390 kA, and the EBW current is 100 kA. The β_N reaches 9.0, with β reaching 42.5%. The peak density is 0.42×10^{20} /m³, li(1) is 0.48, $H_{98(y,2)}$ is 1.55, and the safety factor drops to 1.7 at 3.5 s. The central safety factor crosses 2.0 at 1.6 s, so the descent is quite slow.

When including HHFW, it was assumed to provide only heating as described in Section 3, but no CD, when combined with NBI. The injected power is 4 MW for NBI (at 80 keV), 3 MW for HHFW, and 3 MW for EBW. Here we include higher energy confinement and broader NB current profile. The bootstrap and NB currents are each 430 kA, the EBW current is 100 kA. The β_N reaches 7.7, β exceeds 39%, the safety factor remains above 3.0, the $H_{98(y,2)}$ factor is 1.5, and the peak density is 0.3×10^{20} /m³. The current profile is broad with li(1) at 0.5, the current diffusion time is 750 ms, and the toroidal field flattop available (3.5 s) provides for more than 4 of these relaxation times. The plasma is stable to n=∞ ballooning modes, except in the pedestal region, and n=1 with a wall located at 1.5a on the outboard only. A case is also simulated with narrow NB current profile (like 109070), producing similar results. Results are shown in Fig. 5.

**5. Simulations of Non-solenoidal Current Rampup**

The non-solenoidal initiation and current rampup is considered a critical goal of the ST program since its attractiveness is directly tied to eliminating the OH solenoid on the inboard side of the device and allowing access to compact geometry. This milestone can be divided into 3 primary thrusts: initiation with outer PF coils, and/or Coaxial Helicity Injection (CHI), low I_P rampup phase typically achieved with an RF source due to limitations on confinement of beam ions at low plasma current, and the high I_P rampup phase which would include the use of NBI to end up at an attractive advanced plasma configuration. The time scales required for this type of rampup are long compared to those required with inductive current rampup due to the reliance on bootstrap current along with HHFW (on-axis), EBW (off-axis), and NB (on-axis) non-inductive current drive sources. These restrict the rampup time to be comparable to the on-axis current diffusion time. The formation of a "current hole" might

allow faster ramps if it is stable, however, the drive for this is the time dependent increase in off-axis non-inductive current, which can not be sustained indefinitely. For the present simulations current holes are avoided, which should set the longest time scales required for such a discharge. The available flattop is determined by the TF coil, ranging from 1.5 s at 0.5 T to 5.0 s at 0.3 T.

The simulations assume that the plasma starts the rampup at I_P = 100 kA, provided by the initiation phase, which is treated as inductive current. HHFW is the current drive source in the low Ip phase, and NBI is added in the high Ip phase. The toroidal field is 0.45 T. In the low Ip phase the HHFW power is ramped slowly to avoid current hole formation, while the density is ramped to keep the temperature sufficiently low to access short core current diffusion time scales. In order to keep the temperature from increasing too fast in this phase the plasma is assumed to be limited on the inboard to avoid transition to H-mode. The peak electron temperature reaches 1.3 keV, while the density ramps up to 0.3×10^{20} /m^3 over 0.3 s. The poloidal β reaches 3.0 in this phase since the total plasma current is low. Around 0.3-0.4 s the plasma is diverted, allowing an improvement in global confinement, with the poloidal β reaching 4.0. Then beginning at 0.5s the NBI power is injected accounting for the poor beam ion confinement at lower plasma current. The corresponding total NB driven current is also reduced, based on the beam confinement observed in the I_P rampup in discharge 109070 from TRANSP. The heating and driven current from the beam continue to improve as the plasma current increases. In addition, the poloidal β drops reaching 2.75 by 4.0 s. The $β_N$ reaches about 5.5 during the discharge simulation and relaxes to 5.0 by 4 s. By 2 s (the flattop available at 0.45 T) the total plasma current has reached just over 400 kA, and by 4 s has reached almost 500 kA. The HHFW current begins to drop after 0.5 s due to the rising plasma density and onset of NBI which would provide fast ions to absorb the FW power. Since the beam ions are not well confined over this simulation a significant HHFW current persists. At a fixed radius of 0.9 m, the PF coils link 0.27 V-s. The poloidal magnetic flux at the plasma edge changes by –0.025 Wb, while the flux at the magnetic axis changes by –0.125 Wb, which is opposite to that for inductive current ramp (both edge and axis flux rise for the TSC convention), and is indicative of non-inductive current ramp. These results are shown in Fig. 6. Another simulation of the non-solenoidal rampup was done at the lower toroidal field of 0.35 T, which would allow 3.5 s of flattop. This simulation showed similar behavior to the 0.45 T case, although by 4 s the plasma current reached 440 kA, $β_N$ reached 6.2, and the central safety factor drops to 2.0. It appears that NSTX does not have sufficient pulse length to connect to a high performance plasma configuration, but can demonstrate the critical features of the non-inductive rampup.

Another simulation was performed in which only heating from the HHFW was assumed, which causes the bootstrap current to be the only current drive source, apart from the assistance provided by the PF coils. The plasma current ramped up to approximately 275 kA by 0.5 s, compared to about 350 kA with HHFW CD. The current profile was quite broad, since only bootstrap current is driven non-inductively, with li(1) reaching 0.4 and $β_P$ obtaining 5.6. It is very difficult in the simulation to control the plasma shape which became highly elongated reaching 3.5 due the strong variations in the plasma pressure and current profile. This method would certainly be more susceptible to current hole formation. This does demonstrate the strong coupling of plasma shaping and current profile at low li and will be critical to controlling the discharge evolution for these types of plasmas.
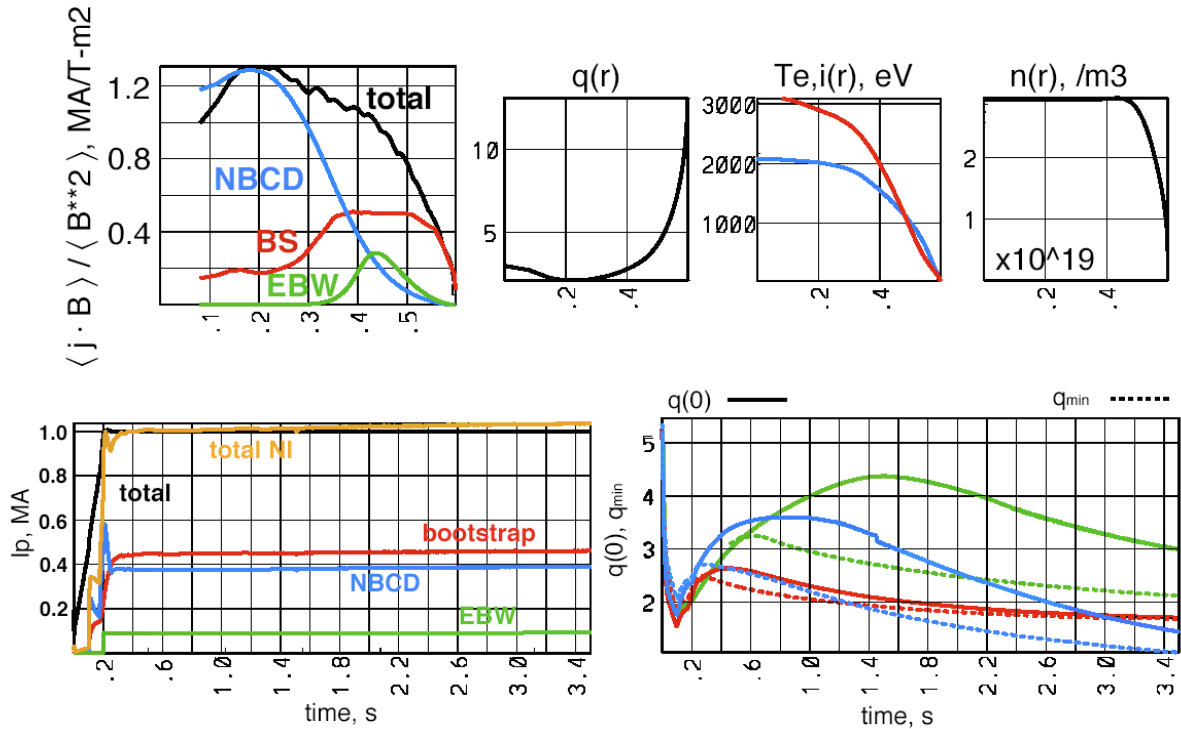
Figure 5. *Time histories of the central and minimum safety factors for 100% non-inductive high β scenarios using only NBI and broad NB current profile (red), using NBI and HHFW with narrow current density (blue) or broad NB current density (green). The profiles and plasma current contributions are shown for the NBI and HHFW with broad NB current density.*
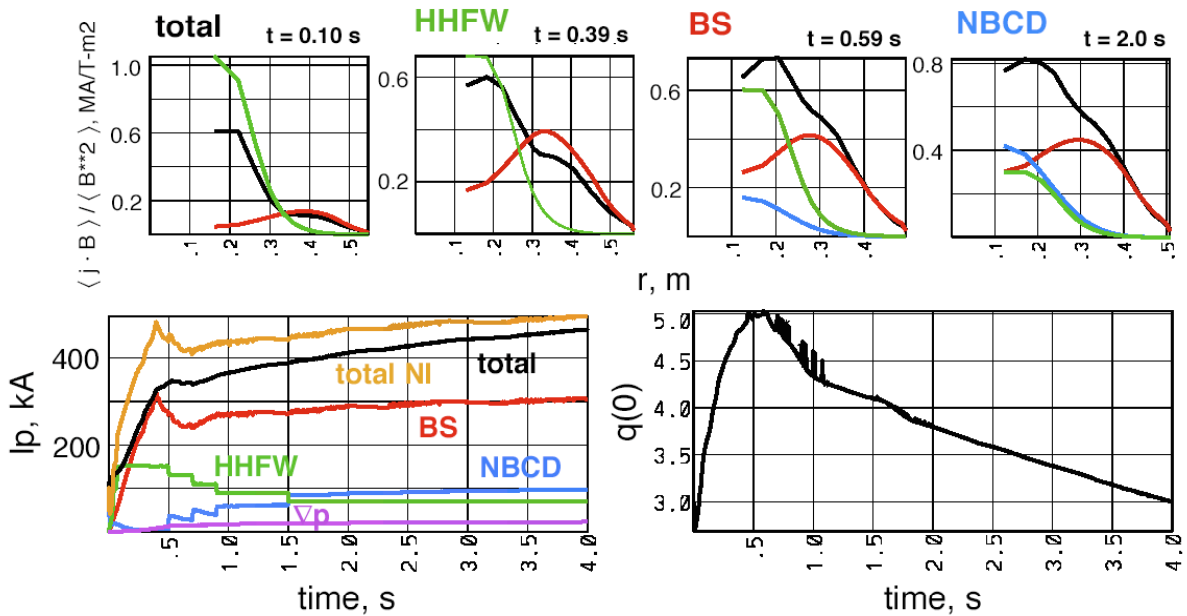
Figure 6. *Time histories from the non-solenoidal current rampup simulation of the plasma current contributions and central safety factor, and parallel current densities at various times. The significant overdrive is apparent in the profiles and plasma current, and long time scales are required to relax.*

6. Conclusions

Simulations of advanced ST plasma scenarios in NSTX using TSC have shown that the 100% non-inductive current, 100% non-inductive high β, and non-solenoidal current rampup milestones can be achieved, based on reasonable extrapolations of existing experimental discharges. The 100% non-inductive scenarios at higher B_T with NBI only or NBI and HHFW achieve bootstrap current fractions over 50% at $I_P = 800$ kA, require energy confinement already achieved on NSTX, and reach β_N and β values of 4.7 and 13%, respectively. The 100% non-inductive high β scenarios at lower B_T with NBI and EBW or NBI, HHFW, and EBW achieve bootstrap current fractions of 50% at $I_P = 1.0$ MA, require energy confinement 10-20% higher than achieved on NSTX, and reach β_N and β values of 7.7-9.0 and 38-43%, respectively. The non-solenoidal current rampup simulations show that NSTX can address the critical features of this technique, addressing many of the challenges for future ST devices without a solenoid. The critical tool upgrades required for access to these plasmas include 1) high elongation (and triangularity) from a modification of the PF1A coils (shown in Fig. 7), 2) control of the density to optimize the external CD efficiencies, 3) development of the EBW system for off-axis CD (shown in Fig. 7), and 4) use of HHFW in non-solenoidal current rampup and in other scenarios to improve their flexibility. The early heating and H-mode transition is found to be important to elevate the safety factor early and prolong scenarios. Other important features are the level of energy confinement achievable, the plasma impurity content, the peakedness of the NB driven current profile, and maintaining the safety factor above 1.5 to avoid a strong internal kink character. Simulations will continue as discharges closer to these advanced ST conditions are produced in the experiment.

References

[1] Ono, M., et al., Nucl. Fusion, **44**, (2004), 452.
[2] M. Peng, et al., this conference.
[3] E. J. Synakowski, et al., Nucl. Fusion, **43**, (2003), 1653.
[4] S. C. Jardin, et al., J. Comp. Phys., **66**, (1983), 481.
[5] R. Budny, et al., Nucl. Fusion, **32**, (1992), 429.
[6] T. K. Mau, et al., "Modeling of Fast Wave Current Drive in Standard and Second Stability Bootstrapped Reactor Plasmas,,, EPS Topical Conference Abstracts on Radiofrequency Heating and Current Drive in Fusion Devices, Brussels, (1992), 181.
[7] R.W. Harvey and M.G. McCoy, Proceedings of the IAEA Technical Committee on Advances in Simulation and Modeling of Thermonuclear Plasmas, Montreal, Quebec (International Atomic Energy Agency, Vienna, 1993), p. 489; USDOC NTIS Doc. No. DE93002962.
[8] G. Taylor, et al., Phys. Plasmas, **11**, (2004), 4733.
[9] J. DeLucia, et al., J. Comp. Phys., **37**, (1980), 183.
[10] J. M. Greene and M. S. Chance, Nucl. Fusion, **21**, (1981), 453.
[11] R. C. Grimm, et al., J. Comp. Phys., **49**, (1983), 94.

External Distribution

Plasma Research Laboratory, Australian National University, Australia

Professor I.R. Jones, Flinders University, Australia

Professor João Canalle, Instituto de Fisica DEQ/IF - UERJ, Brazil

Mr. Gerson O. Ludwig, Instituto Nacional de Pesquisas, Brazil

Dr. P.H. Sakanaka, Instituto Fisica, Brazil

The Librarian, Culham Laboratory, England

Mrs. S.A. Hutchinson, JET Library, England

Professor M.N. Bussac, Ecole Polytechnique, France

Librarian, Max-Planck-Institut für Plasmaphysik, Germany

Jolan Moldvai, Reports Library, Hungarian Academy of Sciences, Central Research Institute
    for Physics, Hungary

Dr. P. Kaw, Institute for Plasma Research, India

Ms. P.J. Pathak, Librarian, Institute for Plasma Research, India

Ms. Clelia De Palo, Associazione EURATOM-ENEA, Italy

Dr. G. Grosso, Instituto di Fisica del Plasma, Italy

Librarian, Naka Fusion Research Establishment, JAERI, Japan

Library, Laboratory for Complex Energy Processes, Institute for Advanced Study,
    Kyoto University, Japan

Research Information Center, National Institute for Fusion Science, Japan

Dr. O. Mitarai, Kyushu Tokai University, Japan

Dr. Jiangang Li, Institute of Plasma Physics, Chinese Academy of Sciences,
    People's Republic of China

Professor Yuping Huo, School of Physical Science and Technology, People's Republic of China

Library, Academia Sinica, Institute of Plasma Physics, People's Republic of China

Librarian, Institute of Physics, Chinese Academy of Sciences, People's Republic of China

Dr. S. Mirnov, TRINITI, Troitsk, Russian Federation, Russia

Dr. V.S. Strelkov, Kurchatov Institute, Russian Federation, Russia

Professor Peter Lukac, Katedra Fyziky Plazmy MFF UK, Mlynska dolina F-2,
    Komenskeho Univerzita, SK-842 15 Bratislava, Slovakia

Dr. G.S. Lee, Korea Basic Science Institute, South Korea

Institute for Plasma Research, University of Maryland, USA

Librarian, Fusion Energy Division, Oak Ridge National Laboratory, USA

Librarian, Institute of Fusion Studies, University of Texas, USA

Librarian, Magnetic Fusion Program, Lawrence Livermore National Laboratory, USA

Library, General Atomics, USA

Plasma Physics Group, Fusion Energy Research Program, University of California
    at San Diego, USA

Plasma Physics Library, Columbia University, USA

Alkesh Punjabi, Center for Fusion Research and Training, Hampton University, USA

Dr. W.M. Stacey, Fusion Research Center, Georgia Institute of Technology, USA

Dr. John Willis, U.S. Department of Energy, Office of Fusion Energy Sciences, USA

Mr. Paul H. Wright, Indianapolis, Indiana, USA